Model Catalyst Studies on Vanadia Particles Deposited onto a Thin-Film Alumina Support. 1. Structural Characterization

Norbert Magg, Javier B. Giorgi, Thomas Schroeder, Marcus Bäumer,* and Hans-Joachim Freund

Fritz-Haber-Institut der Max-Planck-Gesellschaft, Faradayweg 4-6, D-14195 Berlin, Germany

Received: February 19, 2002

A model system of alumina-supported vanadia particles, representing catalysts of the type oxide$_1$/oxide$_2$, was prepared under ultrahigh vacuum (UHV) conditions and characterized regarding its structural and electronic properties. As supporting oxide we used a thin, well-ordered alumina film grown on NiAl(110), which allows the application of scanning tunneling microscopy (STM), infrared reflection−absorption spectroscopy (IRAS), and X-ray photoelectron spectroscopy (XPS) without charging effects. Vanadium oxide particles were prepared via metal evaporation in an oxygen ambient, leading to the growth of small, roundish oxide particles with vanadium in the +3 oxidation state. The particles are shown to interact strongly with the alumina support, resulting in an increased alumina film thickness and a distortion of the alumina film structure. IR absorption signals of the deposits could be successfully assigned to specific V-containing species, thus providing insight into the inner structure of the particles. The species identified are surface-localized vanadyl groups (V=O), interface-localized vibrations involving V, O, and Al ions, and lattice structures typical of bulk V_2O_3.

1. Introduction

Vanadium oxides supported by a second oxide such as TiO_2, SiO_2, or Al_2O_3 represent an important class of active catalysts industrially applied to a variety of reactions. These include oxidation as well as reduction reactions, e.g., the oxidation of *o*-xylene to phthalic anhydride, the oxidation of sulfur dioxide to sulfur trioxide, the ammoxidation of aromatic hydrocarbons, and the selective catalytic reduction of NO_x with ammonia.[1,2] Typically, submonolayer to monolayer quantities of vanadium oxides are dispersed on the substrate using impregnation, grafting, or chemical vapor deposition techniques followed by calcination cycles. Numerous investigations have been dedicated to the role of the support oxide and to the identification of active species. It was found that the choice of the support oxide can influence the activity of a catalyst system by several orders of magnitude.[1,2] The reducibility of the support oxide and the coupling between the support and vanadia, mediated via V−O support bonds, have been proposed to play a decisive role. However, many questions remain unanswered, such as the role of vanadyl groups or of vanadium oxides in an oxidation state lower than +5.[1,2] To obtain a deeper understanding, experiments on model catalyst systems exhibiting a reduced complexity are necessary. In fact, in the past 10 years there have been several studies dealing with the characterization of well-defined model systems prepared under ultrahigh vacuum (UHV) conditions.[3−9] Most of these studies were restricted to the system vanadia/TiO_2(110), and only a limited number of publications on the adsorption and reaction behavior of such systems are available.[8,10,11] Proceeding in this direction, we have investigated a model catalyst system consisting of vanadium oxide particles on an alumina thin-film support. Utilizing scanning tunneling microscopy (STM), X-ray photoelectron spectroscopy (XPS), and infrared (IR) spectroscopy, we are aiming to understand the system from preparation and structural characterization to adsorption and reaction properties. In this first paper, we focus on structural issues, whereas the interaction with gas molecules will be disussed in a forthcoming publication.[12]

2. Experimental Section

The experiments were performed in a multichamber UHV system operated at a base pressure below 2×10^{-10} mbar. Sample preparation as well as XPS and infrared measurements were carried out in one part of the UHV system, whereas STM images were taken in another part. The transfer between these two stages had to be done with the sample kept at room temperature. Consequently, all STM images were generated at this temperature, even though a variable-temperature scanning tunneling microscope (Omicron) was used. Tunneling was performed in constant-current mode with voltages in the range of +2.2 to +3.0 V, i.e., electrons tunneled from filled tip states into empty sample states, and currents around 0.05−0.1 nA. Photoelectron spectra were recorded by a concentric hemispherical analyzer (Scienta SES 200) set to a pass energy of 150 eV. A dual-anode X-ray tube served as an excitation source. Al Kα radiation was chosen to avoid overlap of O 1s and V 2p emissions with Auger signals from the NiAl substrate. Infrared spectra were acquired with a Fourier transform infrared spectrometer (Bruker IFS 66v/S). P-polarized light was coupled into the UHV chamber via viton sealed KBr windows and reflected from the sample surface at an angle of 84°. Spectra were recorded using a liquid nitrogen cooled MCT detector operating in the mid-infrared region at frequencies above 600 cm^{-1}. Typically 4096 scans were accumulated. Spectral resolution after apodization was 3.3 cm^{-1}. For the following it is important to note that the metal surface selection rule applies for the system discussed here. This is due to the limited thickness of the alumina film and the metal substrate underneath. As a result, only structures can be observed in the IR spectra which exhibit

* Corresponding author. Telephone: +49 30 8413 4220. Fax: +49 30 8413 4101. E-mail: baeumer@fhi-berlin.mpg.de.

a nonzero component of the dynamic dipole moment perpendicular to the NiAl substrate.

The preparation of the model catalyst system was carried out in two steps comprising the growth of the alumina thin-film support and the deposition of vanadia particles. The first step comprised the oxidation of a sputter-cleaned NiAl(110) surface at 550 K by exposure to about 3000 L O_2 (1 L = 10^{-6} Torr s) and subsequent annealing at about 1100 K.[13] Usually two oxidation/annealing cycles were employed to ensure complete oxidation of the NiAl surface. This results in a well-ordered alumina film[13] of ~5 Å thickness.[13-15] After the preparation, the oxide film quality was checked by STM and LEED (low-energy electron diffraction). In a second step vanadium (>99.8%, Goodfellow) was deposited by means of an electron-beam evaporator (EFM3T, Focus) in an oxygen ambient of 1×10^{-7} mbar O_2. During vanadium evaporation, the sample was held on a retarding potential to prevent vanadium ions from being accelerated toward the sample. The deposition rate of 0.36 monolayer (ML) per min was determined by means of a quartz crystal microbalance and counterchecked by two-dimensional submonolayer growth on NiAl(110) and subsequent STM measurements. Since the stoichiometry and morphology of the prepared vanadia particles may change with increasing vanadium loading, all coverages cited are expressed in terms of monolayer of vanadium metal deposited. One monolayer of vanadium (1 MLV) as calculated on the basis of the interlayer distance between the close-packed (110) planes of bulk vanadium of 2.14 Å corresponds to 1.54×10^{15} atoms cm^{-2}.

3. Results and Discussion

The results presented are grouped into three sections, dealing with the characterization of the model catalyst system by STM, XPS, and IR spectroscopy, respectively.

3.1. STM Results. Two representative STM images are shown in Figure 1 for vanadia particles grown at a substrate temperature of 300 K: one for the very low coverage of 0.01 MLV and the other for an intermediate coverage of 0.32 MLV. The preparation conditions applied lead to the growth of roundish, but comparatively flat vanadia particles. Their diameter is in the range of 20−30 Å and appears to be coverage independent. It has to be taken into account, however, that tip convolution effects can lead to a substantial overestimation of the particle diameter, especially in the low coverage regime, possibly up to a factor of 2.[16]

The particle height, on the other hand, depends on the vanadia coverage. Upon increasing the coverage from 0.01 to 0.1 MLV, the particle height increases from average values around 3−4 Å to values in the range of 5−6 Å, as extracted from corresponding line scans (Figure 1b shows such a line scan for a 0.01 MLV deposit). For the interpretation of these values, it is important to know that the height measured by STM depends also on the gap voltage. For voltages below ~ +3 V the particle heights are measured with respect to the NiAl surface whereas at voltages higher than ~ +5 V the reference level is located in the surface region of the alumina film. This leads, as demonstrated in Figure 1c, to a change of the apparent particle height by ~4 Å, which is in good agreement with the thickness of the alumina film as determined by other techniques.[14] Similar results have been found previously for the clean alumina film[17,18] and for alumina-supported Pd deposits.[18] Since all our STM images were taken at voltages between +2.2 and +3.0 V, where the image quality usually was superior, the above-mentioned values for the average particle heights are given with respect to the NiAl substrate. Subtracting from these heights the apparent
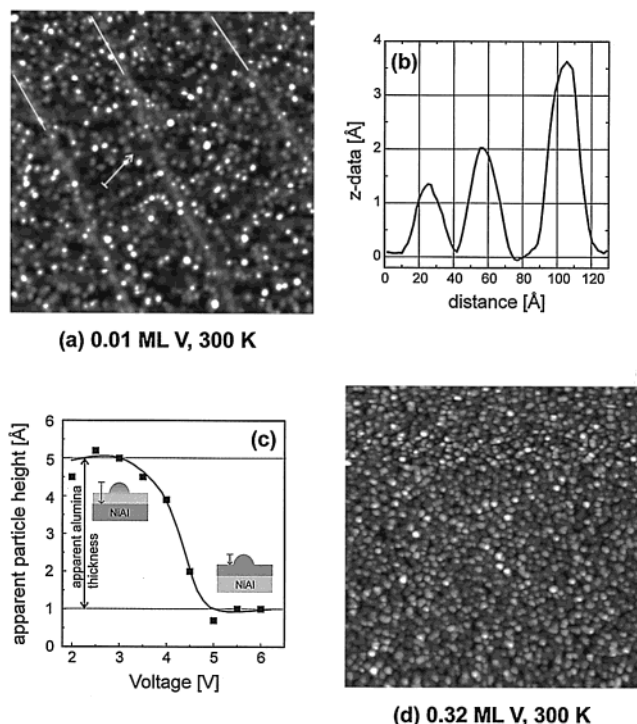

Figure 1. Room-temperature STM images (100 nm × 100 nm) after deposition of vanadium onto a thin alumina film at 300 K in an oxygen ambient. (a) 0.01 MLV (+3.0 V, 0.1 nA). The white lines mark antiphase domain boundaries of the thin-film alumina support. (b) Line scan from image (a) taken along the white arrow. (c) Voltage dependence of the apparent particle height determined at a single vanadia particle from a 0.03 MLV deposition experiment. (d) 0.32 MLV (+2.2 V, 0.07 nA).

height of the alumina film (4 Å) moves the reference level toward the surface of the alumina film and reveals that our vanadia particles are partially incorporated into the surface. This in turn suggests that vanadium deposited in an oxygen environment interacts strongly with the alumina film.

The vanadia particles are homogeneously distributed over the alumina support. In particular, no preferential growth was found at the line defects of the alumina substrate as has been observed in previous studies for metal particles, such as Rh and Pd.[14] The most prominent line defect type on the alumina film are antiphase domain boundaries which are visible in Figure 1a as protruding lines running parallel to each other at a distance of about 100−200 Å. They represent the nucleation centers with the deepest potential well. Another type of nucleation centers present on the surface are point defects. Although these defects could not be directly imaged by STM, their number density was determined by comparative nucleation studies to be about 1×10^{13} cm^{-2}.[19,20] Depending on the predominant nucleation site, characteristic curves for the particle number densities as a function of the metal coverage have been determined. Which nucleation site actually dominates is crucially affected by the diffusion length of the metal atoms on the substrate, i.e., by the substrate temperature and the interaction strength between metal and oxide film. Figure 2 shows a comparison of the corresponding data for vanadia particles with results from our previous metal nucleation studies. It can be seen that vanadia particles grow with a significantly higher number density as compared to all other cases examined. This observation suggests that the interaction of vanadium atoms with the surrounding oxygen ambient decreases their diffusion length on alumina to such an extent that nucleation is mainly restricted to regular surface sites. This is reflected in the low average number of
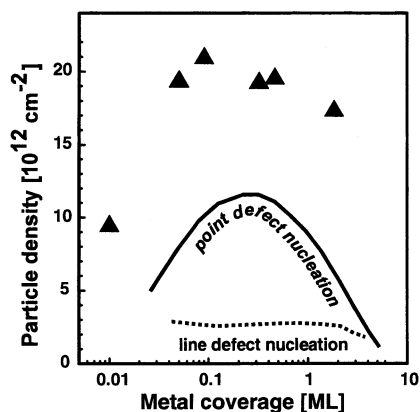
8758 *J. Phys. Chem. B, Vol. 106, No. 34, 2002*

Magg et al.

Figure 2. Development of vanadia particle number density as a function of vanadium metal coverage. The particle number density was determined by counting the particles in several STM images and averaging the area-normalized values. Furthermore, curves are shown which are typical of metal nucleation on line defects and point defects as determined from our previous work on Rh, Pd, Ir, Pt, and Co particles.[14]
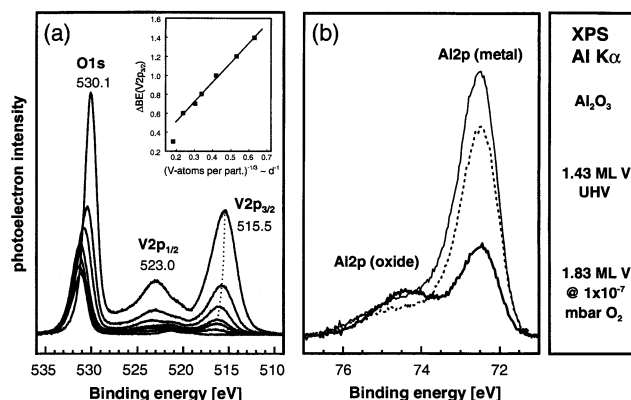

Figure 3. Al Kα excited XP spectra of room-temperature-grown vanadia particles on a thin alumina film. (a) O 1s and V 2p photoelectron emissions for increasing vanadium loading (0, 0.18, 0.32, 0.46, 0.92, 1.83, and 18.3 MLV). The inset illustrates the linear correlation between binding energy shift and reciprocal particle diameter, the latter being proportional to the expression (number of vanadium atoms per particle)$^{-1/3}$. (b) Al 2p photoelectron emissions from aluminum in a metallic and an oxidic environment. The signal from the clean alumina film (thin line) is compared to two different room-temperature preparations, one where vanadium is deposited under UHV conditions (dotted line) and one where vanadium is deposited in an oxygen ambient (thick line).

vanadium atoms per particle, being 1−2 and 25 for the two different vanadium coverages shown in Figure 1.

Similar results are found in experiments where the substrate temperature was changed to 90 K; i.e., also at this temperature homogeneously distributed, roundish oxide particles were observed which nucleate on regular surface sites.

That oxygen indeed plays an important role for the nucleation behavior is corroborated by investigations dealing with the growth of vanadium under UHV conditions. In this case, lower particle number densities which are in accordance with point defect nucleation have been found.[21,22] An important question, of course, is whether the vanadium atoms are oxidized in the gas phase during their way from the evaporation source to the substrate or after deposition on the surface. Considering the low partial pressure of oxygen during the preparation, the system certainly is in the molecular flow regime where intermolecular collisions are no longer important. Thus, the reaction between vanadium and oxygen should occur only after condensation of vanadium on the substrate. In contrast to that, experiments are reported in the literature where vanadia cluster were successfully generated in the gas phase by exposure to oxygen partial pressures in a region of 1 mbar.[23−25]

3.2. XPS Results. The electronic properties of the vanadia/alumina system were investigated by XPS experiments using Al Kα radiation as an excitation source. Two different binding energy regimes are of particular interest: the region between 510 and 535 eV where photoelectrons from O 1s and V 2p core levels are observed, providing information on the oxidation state of the vanadia particles, and the region between 70 and 78 eV where photoemission signals from the Al 2p substrate levels are found.

In Figure 3a, O 1s and V 2p features are displayed as a function of the vanadium coverage. The clean alumina film is characterized by an O 1s signal at 531.1 eV (small X-ray satellite features (Al Kα$_{3,4}$) which are shifted to lower binding energies (BE) by 9.5−11.7 eV are also observed[26]). Upon vanadium deposition, the intensity of the oxygen signal increases, indicating the formation of an oxidized vanadium overlayer. Its position shifts to a value of 530.1 eV at the highest coverage examined (18.3 ML) where no emission signals originating from the alumina substrate can be detected anymore. The corresponding values found in the literature for vanadium oxides at room temperature are 530.1 (V$_2$O$_3$), 529.9 (VO$_2$), and 529.8 eV (V$_2$O$_5$).[27]

The two peaks growing with increasing amount of vanadium deposited result from the two spin−orbit splitted V 2p components. Since the V 2p$_{1/2}$ signal overlaps with O 1s satellite features, only the V 2p$_{3/2}$ emission was used for the analysis. After formation of multilayer amounts of vanadia, its binding energy is 515.5 eV. Comparing this number to the literature[27] − 515.7 (V$_2$O$_3$), 516.2 (VO$_2$), and 516.9 eV (V$_2$O$_5$) − it is obvious that, at high coverages, vanadia grows with an oxidation state close to +3. At low coverages, however, the V 2p$_{3/2}$ signal is shifted to higher binding energies, suggesting at first glance that smaller particles grow with a higher oxidation state. However, final state effects are known to result in similar size-dependent BE shifts for small conducting particles on insulating substrates.[28] This is due to the Coulomb interaction between the leaving photoelectron and the positively charged particle. As many lower valence vanadium oxides, such as V$_2$O$_3$, are metallic at 300 K, such considerations apply here as well. By plotting the binding energy shift versus the (number of vanadium atoms per particle)$^{-1/3}$, a quantity that is inversely proportional to the particle diameter, a linear correlation is obtained, revealing that it is indeed the Coulomb contribution in the final state[28] and not an increasing oxidation state which is decisive in the present case (see inset of Figure 3a). The breakdown of this linear relationship for the largest particles is probably due to the onset of coalescence.

In conclusion, the data show that, at low coverage, the observed BE shift is dominated by final state contributions. At higher coverages, however, the BE detected for O 1s and V 2p$_{3/2}$ point toward an oxidation state of vanadia close to +3. This idea is supported by NEXAFS (near edge X-ray absorption fine structure) measurements of vanadia particles prepared under identical conditions on Al$_2$O$_3$(0001) where the formation of V$_2$O$_3$ overlayers also in the regime of low vanadium coverages was reported.[29] Furthermore, vanadia in the oxidation state +3 turns out to be the oxide that preferentially grows under typical UHV conditions such as those applied in the present study. Even the choice of the substrate seems to have only a minor impact on the oxidation state as deduced from corresponding experiments found in the literature: Cu(110),[30] Au(111),[31,32] W(111),[33]

Alumina-Supported Vanadia Particles

J. Phys. Chem. B, Vol. 106, No. 34, 2002 **8759**

and TiO$_2$(110).[3] It is important to note, however, that the structure of the vanadia overlayer prepared in this way does not necessarily reflect the bulk V$_2$O$_3$ structure. Photoelectron diffraction measurements of the system vanadia/TiO$_2$(110), for instance, revealed that the vanadia overlayer grows in a substrate stabilized rutile structure with an epitaxial relationship to the TiO$_2$(110) surface.[34]

Figure 3b shows XP spectra in the range of Al 2p photoelectrons. The spectrum from the clean alumina substrate is dominated by an Al 2p signal at 72.5 eV originating from metallic aluminum in the NiAl substrate. Al 2p electrons from the Al$_2$O$_3$ film give rise to a broad shoulder on the high binding energy side at about 75.0 eV. Upon deposition of vanadium metal under UHV conditions, both features are attenuated in the same way, thus preserving a constant intensity ratio. However, during vanadia preparation in an oxygen ambient, the metallic part of the Al 2p signal is substantially decreased while the oxide signal is enhanced. The obvious explanation for this change in the ratio between oxidized and metallic aluminum is an increase of the alumina film thickness. Since the clean alumina film is absolutely inert with respect to a further reaction with oxygen under the conditions applied, the vanadia particles have to act as an oxidation catalyst, in agreement with what has already been observed for higher deposition temperatures.[21] A similar but less pronounced catalytic behavior has recently been found for Pd particles supported on the same substrate after exposure to an O$_2$ atmosphere.[35]

In an attempt to reduce the interaction between vanadia and alumina, an experiment was carried out where vanadium was deposited at low temperature (100 K) but at the same oxygen partial pressure. As expected (not shown), this reduces the above-described effect significantly. The V 2p$_{3/2}$ signal is shifted to higher binding energy as compared to room-temperature deposits of comparable size, indicating that more oxygen is bound now in the vanadia particles. However, as soon as the sample is heated to 300 K, the V 2p$_{3/2}$ peak shifts back to lower BE. From our previous studies on metal particles we know that sintering effects are negligible in this temperature range.[14] This is especially true for vanadia particles which interact much stronger with the alumina film than all the metals examined so far. Thus the observed peak shift is not connected to changes in the particle size, which again would involve final state effects, but is caused by a reduction of vanadia. At the same time, the oxide derived Al 2p signal increases, indicating that there is a transfer of oxygen from the vanadia particles to the NiAl substrate.

3.3. IRAS Results. In Figure 4a IR spectra are shown for a complete vanadia coverage series. For the clean alumina film several surface optical phonons can be observed, the most prominent of which is located at 866 cm^{-1}. With increasing amount of vanadia deposited, this feature gets attenuated very rapidly, once again confirming the strong interaction between the vanadia deposits and the alumina support. At the same time new features appear in the IR spectra. At the highest vanadium coverage examined, three absorption bands are visible whose frequencies ν and full widths at half-maximum (fwhm) are listed in Table 1. In addition, some intensity remaining from the strongest alumina phonon is still visible as a shoulder on the low-energy side of the band at 945 cm^{-1}. Comparison to the situation found after deposition of vanadium under UHV conditions, as presented in Figure 4b for two different vanadium coverages, reveals that the perturbation of the substrate structure is much more severe for the vanadia deposits. This is in perfect agreement with LEED observations. In the case of vanadia
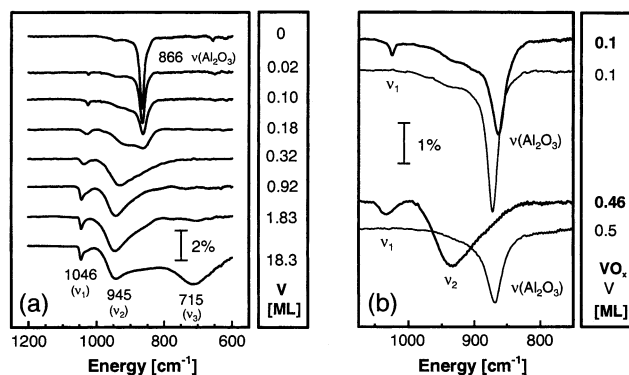

Figure 4. (a) IR spectra taken at 300 K for a vanadia coverage series. (b) Comparison of room-temperature IR spectra for particles prepared under UHV conditions (V, thin line) and in an oxygen ambient (VO$_x$, thick line). All spectra are referenced to spectra from clean NiAl taken at the corresponding temperature.

TABLE 1: Frequencies (ν) and Full Width at Half-Maximum (fwhm) for the Three Oxide Vibrations Identified in Figure 4a, Bond Length, and Bond Order[a]

	ν/cm^{-1}	fwhm/cm^{-1}	bond length/Å	bond order
ν_1	1046	13	1.57	1.96
ν_2	945	110	1.63	1.62
ν_3	715	120	1.77	1.06

[a] Values for the bond length and the bond order of the three species were calculated on the basis of empirical relations published in ref 39.

particles, the characteristic diffraction pattern of the alumina substrate disappears already after deposition of about 0.2−0.3 MLV, whereas it is still visible in the case of metallic vanadium particles prepared by evaporation of 1 MLV.

The new bands observed in Figure 4a are not present in the spectra of metallic vanadium particles and must therefore be attributed to V-containing oxide vibrations. A closer look at their intensity evolution shows that the two bands at higher energy saturate after a vanadium deposition of about 1 MLV. The vanadium−oxygen species giving rise to these bands are consequently localized either at the surface of the particles or at their interface to the alumina substrate. The third band at 715 cm^{-1} appears later and grows with increasing amount of vanadia. In fact, only for the highest coverage examined here can it be unambiguously identified. This behavior suggests the presence of a bulk species.

A definite assignment of the IR absorption bands is possible by a comparison with literature data. The most detailed information is available for V$_2$O$_5$ single crystals where a complete normal coordinate analysis has been carried out, rendering an assignment of transverse and longitudinal optical frequencies (TO and LO) to specific vanadium−oxygen bonds possible.[36,37] However, since our IR absorption data originate from nanometer-sized and most likely amorphous particles, a comparison with results derived from measurements on single crystals might be misleading. In particular, there should be no TO−LO splitting present in our case. It turns out that powder samples and supported vanadia catalysts, where molecularly dispersed species are prepared by wet impregnation or grafting techniques, bear the closest resemblance to the structures found on our samples.[2,38] Thus, a first quantitative classification of the bands observed can be achieved on the basis of an empirically developed correlation between Raman stretching frequencies and crystallographically determined bond lengths.[39] This so-called Hardcastle−Wachs model is expected to be generally applicable to all vanadates if medium-range order is absent. Using these empirical expressions, values for the V−O

bond lengths and bond orders can be calculated (see Table 1), motivating the following band assignments.

According to Table 1, the **band ν_1** represents a species in which vanadium and oxygen form a double bond, i.e., a vanadyl group (V=O). On supported vanadia catalysts they are routinely found and are considered to play a decisive role.[38,40,41] Since vanadyl groups prefer end-standing positions, one expects them to be localized at the surface of the particles. This is proven in a forthcoming publication,[12] where adsorbed CO is shown to interact with V=O. Surprisingly, vanadyl groups are not a structure element of bulk truncated V_2O_3 surfaces. On the other hand, similar observations have been made for vanadium oxide layers of different stoichiometry grown on Pd(111),[42] as well as for Cr_2O_3(0001)/Cr(110) films which grow in an isostructural corundum phase and which are terminated by chromyl groups (Cr=O), after the surface has been exposed to O_2.[43] Accordingly, surface-localized double-bonded oxygen does not seem to be an untypical feature of early transition metal oxides prepared under UHV conditions.

A bond order close to 1, as calculated for the **band ν_3**, is typical for the asymmetric stretching vibrations of a single bridge species (V−O−V).[44] The fact that vanadium oxides in an oxidation state close to +3 can indeed exhibit bands around 715 cm^{-1} was proven by HREELS (high-resolution electron energy loss spectroscopy) studies on VO$_x$/Pd (111) inverse catalysts, where strong absorption bands between 630 and 740 cm^{-1} were shown to be characteristic for a bulk V_2O_3 like phase.[42] Whether the species on our sample are present in a linear or in a bent configuration could, in principle, be decided on the basis of IR selection rules by monitoring the frequency region of the corresponding symmetric stretching vibration: in an isotropic surrounding the symmetric stretching frequency should be IR-inactive for a linear configuration and IR-active for a bent one. Unfortunately, this frequency region is below our detection limit.

An assignment of the **band ν_2** at 945 cm^{-1} is more complicated. For powder samples no suitable absorption bands have been reported and the bands found in this frequency regime on supported vanadium oxide catalysts are attributed either to V=O groups in chains of polyvanadate ions[40] or to protonated VO$_2$ or VO$_3$ functionalities.[44] Both explanations are not very likely in our case since neither vanadate ions nor OH groups, which are necessary to form protonated species, are present in our model system.

However, since we know from the saturation behavior of the band ν_2 that the corresponding species could be localized at the interface to the alumina substrate, it is conceivable that we are not dealing with a pure V−O species but with a species involving V, O, and Al. In the case of alumina-supported vanadia catalysts, the formation of AlVO$_4$ species has been suggested to be the origin of bands around 951−965 cm^{-1}.[45] Infrared spectroscopic and crystallographic investigations on AlVO$_4$ powder samples identified absorption bands around 950 cm^{-1} (fwhm ∼ 130 cm^{-1}) which were ascribed to the vibrations of tetrahedral VO$_4$ groups.[46] A strong coupling to Al−O vibrations was reported to be responsible for the blue shift of about +100 cm^{-1} as compared to the more isolated VO$_4^{3-}$ groups in orthovanadates.

To verify the idea that the band at 945 cm^{-1} is connected to an interface-localized species, we have studied the properties of this band as a function of the deposition and measurement temperature. In the upper part of Figure 5, IR spectra are shown for vanadia particles (0.92 MLV) grown at 300 K. Spectra were taken at this temperature and after a subsequent cooling to 90
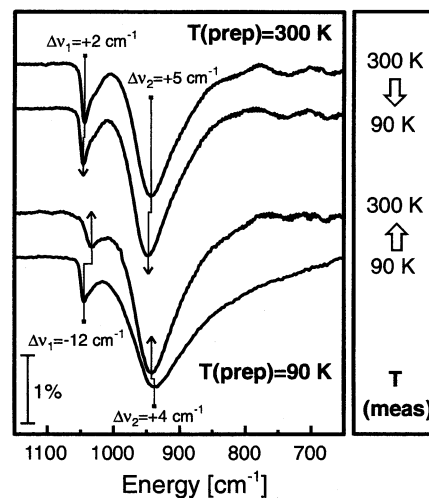

Figure 5. IR spectra for vanadia particles prepared at two different temperatures, T(prep), 300 (top) and 90 K (bottom). After taking spectra at T(prep), the samples were cooled/heated to the complementary temperature, 90 (top) and 300 K (bottom). All spectra are referenced to spectra from clean NiAl at the corresponding temperature.

K. Since this thermal treatment involves no morphological changes, the blue shift observed for the two absorption bands ($\Delta\nu_1 = +2$ cm^{-1}, $\Delta\nu_2 = +5$ cm^{-1}) is only due to a stiffening of the corresponding bonds. These findings underline the assignment of ν_1 to a more isolated species (V=O), whereas the species ν_2 seems to be in closer contact with the alumina substrate whose most intense phonon also shifts by +5 cm^{-1} under the same thermal treatment.

In the lower part of Figure 5, spectra are shown for the reversed experiment, where the same amount of vanadium was deposited at 90 K and then heated to 300 K. Now the observed frequency shifts ($\Delta\nu_1 = -12$ cm^{-1}, $\Delta\nu_2 = +4$ cm^{-1}) reflect not only the reaction of the system to the thermal treatment, i.e., a softening of the corresponding bonds, but also morphological changes. From the XPS results discussed in section 3.2, we know that these changes are connected with an intensified particle−support interaction manifesting itself in an increased alumina film thickness and a reduction of the vanadia particles. The oxygen transferred from vanadia to alumina in the course of this process must at least partially originate from vanadyl groups as deduced from the intensity loss of the band ν_1. The large frequency shift of −12 cm^{-1} points in the same direction. Decreasing dipole−dipole interactions are probably responsible for this red shift, in analogy to the well-known coverage-dependent shifts found for CO adsorbed on metal surfaces.[47] Very similar results have been published on supported vanadia catalysts.[38]

As shown in the lower part of Figure 5, the peak height of the band ν_2 increases upon heating the 90 K deposits to 300 K, implying a growth of the corresponding species as a consequence of the morphological changes under discussion. This is in agreement with the blue shift observed for this band (from Figure 4a we know that the band ν_2 shifts to higher energies while its intensity is growing) which overcompensates the thermally induced red shift.

The behavior of the shoulder on the low-energy side of ν_2 points in the same direction. It reflects some remaining intensity of the strongest alumina phonon and is significantly enhanced in the case where vanadia deposition was carried out at 90 K as compared to the 300 K preparation. Obviously, the alumina film structure is less perturbed under these conditions. However,

Alumina-Supported Vanadia Particles

J. Phys. Chem. B, Vol. 106, No. 34, 2002 **8761**

as soon as the sample is heated, the particle−support interaction increases and the alumina phonon vanishes.

These changes, together with the XPS results, show that the species giving rise to the absorption band at 945 cm^{-1} is interface-localized and involves a vibration of V, O, and Al ions. Although the exact structure cannot be determined, VO_4 tetrahedra coupled to alumina entities as found for $AlVO_4$[46] seem to be a reasonable proposal. At least a simple Al−O−V configuration across the oxygen terminated alumina surface is unlikely, since no such signals are observed in the case where small amounts of vanadium are deposited under UHV conditions (compare Figure 4b) which are known to be in an oxidized state as well.[21] Accordingly, additional oxygen from the gas phase is necessary to form the observed structure.

In conclusion, the three absorption bands observed in the IR spectra are assigned to surface-localized vanadyl groups (ν_1), to interface-localized species comprising V, O, and Al ions (ν_2), and to (V−O−V) bridging structures as they have been found for bulklike V_2O_3 layers (ν_3).

4. Summary and Conclusion

Utilizing STM, XPS, and IR spectroscopy, we have characterized a model catalyst system being composed of vanadia particles supported by a thin alumina film grown on NiAl(110). Preparation of the particles was carried out via evaporation of vanadium in an oxygen ambient of 1×10^{-7} mbar O_2. The conclusions we arrived at can be summarized as follows: According to STM, the preparation conditions applied lead to roundish oxide particles with diameters in the range of 20−30 Å. They grow with a comparatively high number density of about 2×10^{13} particles cm^{-2} and are found to be partially incorporated into the alumina film. XPS and IRAS evidence a strong particle−support interaction eventually leading to an increased alumina film thickness in connection with a significant perturbation of the alumina film structure. The oxidation state of the particles, as deduced from XP spectra, is close to +3. In line with that, we observe an oxide vibration signal in our IR spectra which is compatible to a bulk V_2O_3 structure. Two further vibrational features were assigned to surface-localized vanadyl groups (V=O) and to an interface-localized species comprising V, O, and Al ions.

References and Notes

(1) Bond, G. C.; Tahir, S. F. *Appl. Catal.* **1991**, *71*, 1.
(2) Deo, G.; Wachs, I. E.; Haber, J. *Crit. Rev. Surf. Chem.* **1994**, *4*, 141.
(3) Zhang, Z.; Henrich, V. E. *Surf. Sci* **1992**, *277*, 263.
(4) Negra, M. D.; Sambi, M.; Granozzi, G. *Surf. Sci.* **1999**, *436*, 227.
(5) Guo, Q.; Lee, S.; Goodman, D. W. *Surf. Sci.* **1999**, *437*, 38.
(6) Madix, R. J.; Biener, J.; Bäumer, M.; Dinger, A. *Faraday Discuss.* **1999**, *114*, 67.
(7) Biener, J.; Bäumer, M.; Madix, R. J. *Surf. Sci.* **1999**, *432*, 178.
(8) Wang, Q.; Madix, R. J. *Surf. Sci.* **2001**, *474*, L213.
(9) Chang, Z.; Piligkos, S.; Moller, P. J. *Phys. Rev. B* **2001**, *64*, 165410.
(10) Wong, G. S.; Kragten, D. D.; Vohs, J. M. *Surf. Sci.* **2000**, *452*, L293.
(11) Wang, Q.; Madix, R. J. *Surf. Sci.* **2002**, *496*, 51.
(12) Magg, N.; Giorgi, J. B.; Schroeder, T.; Bäumer, M.; Freund, H.-J. Manuscript in preparation.
(13) Jaeger, R. M.; Kuhlenbeck, H.; Freund, H.-J.; Wuttig, M.; Hoffmann, W.; Franchy, R.; Ibach, H. *Surf. Sci.* **1991**, *259*, 235.
(14) Bäumer, M.; Freund, H.-J. *Prog. Surf. Sci.* **1999**, *61*, 127.
(15) Stierle, A.; Renner, F.; Streitel, R.; Dosch, H. *Phy. Rev. B* **2001**, *64*, 165413.
(16) Stempel, S.; Bäumer, M.; Freund, H.-J. *Surf. Sci.* **1998**, *402−404*, 424.
(17) Bertrams, Th.; Brodde, A.; Neddermeyer, H. *J. Vac. Sci. Technol., B* **1994**, *12*, 2122.
(18) Hojrup Hansen, K.; Worren, T.; Laegsgaard, E.; Besenbacher, F.; Stensgaard, I. *Surf. Sci.* **2001**, *475*, 96.
(19) Libuda, J.; Winkelmann, F.; Bäumer, M.; Freund, H.-J.; Bertrams, Th.; Neddermeyer, H.; Müller, K. *Surf. Sci.* **1994**, *318*, 61.
(20) Frank, M.; Bäumer, M. *Phys. Chem. Chem. Phys.* **2000**, *2*, 3723.
(21) Bäumer, M.; Biener, J.; Madix, R. J. *Surf. Sci.* **1999**, *432*, 189.
(22) Magg, N.; Giorgi, J. B.; Frank, M.; Schroeder, T.; Bäumer, M.; Freund, H.-J. To be published.
(23) Nieman, G. C.; Parks, E. K.; Richtsmeier, S. C.; Liu, K.; Pobo, L. G.; Riley, S. J. *High. Temp. Sci.* **1986**, *22*, 115.
(24) Foltin, M.; Stueber, G. J.; Bernstein, E. R. *J. Chem. Phys.* **1999**, *111*, 9577.
(25) Bell, R. C.; Zemski, K. A.; Justes, D. R.; Castleman, A. W., Jr. *J. Chem. Phys.* **2001**, *114*, 798.
(26) Klauber, C. *Surf. Interface Anal.* **1993**, *20*, 703.
(27) Sawatzky, G. A.; Post, D. *Phys. Rev. B* **1979**, *20*, 1546.
(28) Wertheim, G. K. *Z. Phys. B* **1987**, *66*, 53.
(29) Biener, J.; Bäumer, M.; Madix, R. J.; Liu, P.; Nelson, E. J.; Kendelewicz, T.; Brown, G. E., Jr. *Surf. Sci* **1999**, *441*, 1.
(30) Kishi, K.; Hirai, K.; Yamamoto, T. *Surf. Sci.* **1993**, *290*, 309.
(31) Lewis, K. B.; Oyama, S. T.; Somorjai, G. A. *Surf. Sci.* **1990**, *233*, 75.
(32) Dupuis, A.-C.; Kuhlenbeck, H.; Freund, H.-J. To be published.
(33) Dupuis, A.-C.; Kuhlenbeck, H.; Freund, H.-J. To be published.
(34) Sambi, M.; Della Negra, M.; Granozzi, G. *Surf. Sci.* **2000**, *470*, L116.
(35) Shaikhutdinov, S.; Heemeier, M.; Hoffmann, J.; Meusel, I.; Richter, B.; Bäumer, M.; Kuhlenbeck, H.; Libuda, J.; Freund, H.-J.; Oldman, R.; Jackson, S. D.; Konvicka, C.; Schmid, M.; Varga, P. *Surf. Sci.* **2002**, *501*, 270.
(36) Clauws, P.; Vennik, J. *Phys. Status Solidi B* **1976**, *76*, 707.
(37) Clauws, P.; Broeckx, J.; Vennik, J. *Phys. Status Solidi B* **1985**, *131*, 459.
(38) Wachs, I. E. *Catal. Today* **1996**, *27*, 437.
(39) Hardcastle, F. D.; Wachs, I. E. *J. Phys. Chem.* **1991**, *95*, 5031.
(40) Went, G. T.; Oyama, S. T.; Bell, A. T. *J. Phys. Chem.* **1990**, *94*, 4240.
(41) Busca, G.; Centi, G.; Marchetti, L.; Trifiro, F. *Langmuir* **1986**, *2*, 568.
(42) Sock, M.; Surnev, S.; Ramsey, M. G.; Netzer, F. P. *Top. Catal.* **2001**, *14*, 15.
(43) Seiferth, O.; Wolter, K.; Dillmann, B.; Klivenyi, G.; Freund, H.-J.; Scarano, D.; Zecchina, A. *Surf. Sci.* **1999**, *421*, 176.
(44) Deo, G. Molecular Engineering of Supported Vanadium Oxide Catalysts. Thesis, Lehigh University, Bethlehem, PA, 1992.
(45) Miyata, H.; Fujii, K.; Ono, T.; Kubokawa, Y.; Ohno, T.; Hatayama, F.] *J. Chem. Soc., Faraday Trans. 1* **1987**, *83*, 675.
(46) Baran, E. J.; Botto, I. L. *Monatsh. Chem.* **1977**, *108*, 311.
(47) Hoffmann, F. M. *Surf. Sci. Rep.* **1983**, *3*, 107.